

Optimizing Landsat time series length for regional mapping of lidar-derived forest structure



Douglas K. Bolton^{a,*}, Piotr Tompalski^a, Nicholas C. Coops^a, Joanne C. White^b, Michael A. Wulder^b, Txomin Hermosilla^b, Martin Queinnec^a, Joan E. Luther^c, Olivier R. van Lier^c, Richard A. Fournier^d, Murray Woods^e, Paul M. Treitz^f, Karin Y. van Ewijk^f, George Graham^g, Lauren Quist^g

^a Integrated Remote Sensing Studio, Department of Forest Resources Management, University of British Columbia, 2424 Main Mall, Vancouver, BC V6T1Z4, Canada

^b Canadian Forest Service (Pacific Forestry Centre), Natural Resources Canada, 506 West Burnside Road, Victoria, BC V8Z1M5, Canada

^c Canadian Forest Service (Atlantic Forestry Centre), Natural Resources Canada, 26 University Drive, P.O. Box 960, Corner Brook, Newfoundland and Labrador A2H 6J3, Canada

^d Département de géomatique appliquée, Centre d'Applications et de Recherches en Télédétection (CARTEL), Université de Sherbrooke, Québec J1K 2R1, Canada

^e Ontario Ministry of Natural Resources and Forestry, North Bay, Ontario P1A 4L7, Canada

^f Department of Geography and Planning, Queen's University, 68 University Avenue, Kingston, ON K7L 3N6, Canada

^g Hearst Forest Management, 1589 Front Street, Hearst, Ontario P0L 1N0, Canada

ARTICLE INFO

Editor: Jing M. Chen

Keywords:

Remote sensing
Airborne laser scanning
Enhanced forest inventory
Forest structure
Landsat time series

ABSTRACT

The value of combining Landsat time series and airborne laser scanning (ALS) data to produce regional maps of forest structure has been well documented. However, studies are often performed over single study areas or forest types, preventing a robust assessment of the approaches that produce the most accurate estimates. Here, we use Landsat time series data to estimate forest attributes across six Canadian study sites, which vary by forest type, productivity, management regime, and disturbance history, with the goal of investigating which spectral indices and time series lengths yield the most accurate estimates of forest attributes across a range of conditions. We use estimates of stand height, basal area, and stem volume derived from ALS data as calibration and validation data, and develop random forest models to estimate forest structure with Landsat time series data and topographic variables at each site. Landsat time series predictors, which were derived from annual gap-free image composites, included the median, interquartile range, and Theil Sen slope of vegetation indices through time. To investigate the optimal time series length for predictor variables, time series length was varied from 1 to 33 years. Across all six sites, increasing the time series length led to improved estimation accuracy, however the optimal time series length was not consistent across sites. Specifically, model accuracies plateaued at a time series length of ~15 years for two sites ($R^2 = 0.67\text{--}0.74$), while the accuracies continued to increase until the maximum time series length was reached (24–29 years) for the remaining four sites ($R^2 = 0.45\text{--}0.70$). Spectral indices that relied on shortwave infrared bands (Tasseled Cap Wetness and Normalized Burn Ratio) were frequently the most important spectral indices. Adding Landsat-derived disturbance variables (time since last disturbance, type of disturbance) did not meaningfully improve model results; however, this finding was largely due to the fact that most recently disturbed stands did not have predictions of forest attributes from ALS, so disturbed sites were poorly represented in the models. As model accuracies varied regionally and no optimal time series length was found, we provide an approach that can be utilized to determine the optimal time series length on a case by case basis, allowing users to extrapolate estimates of forest attributes both spatially and temporally using multispectral time series data.

1. Introduction

Forest inventories remain a cornerstone of sustainable forest

management, providing information needs from broad-view strategic planning to operational and tactical forest operation decisions (Kangas and Maltamo, 2006). Spatially explicit information on forest attributes

* Corresponding author.

E-mail address: dbolt@ubc.edu (D.K. Bolton).

inform these forest inventories by providing critical information at multiple spatial and temporal scales (White et al., 2014a). In Canada, the diverse and extensive nature of forest resources has led to the development and application of numerous inventory approaches. Based upon forest stewardship responsibilities, forest inventories are implemented and maintained by provincial or territorial jurisdiction, typically utilizing aerial imagery acquisition and interpretation informed by ground sampling (Leckie and Gillis, 1995). In contrast, to enable systematic characterization and reporting on Canada's forests for national and international reporting, sample based approaches are implemented using photo plots from air photos or high spatial resolution satellite imagery. Over Canada's more accessible and commercially utilized southern forests, air photos are often available, whereas through the largely unmanaged northern extents of Canada's forests, satellite data is availed upon (Wulder et al., 2007). Regardless of the approach, forest inventories remain costly and time consuming to produce, and as a result, many existing forest inventories are over 20 years old. Forest inventories of variable coverage and vintage increase uncertainty in forest management for issues such as estimating future timber availability, as well as responding to communities requiring information on the additional ecological goods and services these forest provide. Detailed and spatially explicit information generated retrospectively can also provide a baseline for understanding forest change (White et al., 2017b) as well as assessing the impacts of changing climate on forest production, stresses, and future vulnerabilities (Price et al., 2013).

The past decade has seen notable developments in a number of remote sensing technologies which have provided new avenues for producing and updating forest inventories with greater efficiency and accuracy (White et al., 2016). With respect to new types of forest inventory data, airborne laser scanning (ALS), also called light detection and ranging (lidar), technologies have revolutionized the capture of three-dimensional forest structure information which can be used more readily in forest inventories over coarser spatial scales than field based methods (Lim et al., 2003). As a result, the application of ALS has grown exponentially across many jurisdictions globally, with forest attribute estimates produced that can meet inventory accuracy requirements (Magnussen et al., 2012). In Canada, ALS acquisitions are typically targeted to specific forest management areas, with only a few jurisdictions having more systematic ALS acquisition programs (Coops et al., 2016). These acquisitions often represent a patchwork of area coverage, with varying data acquisition parameters, data characteristics (e.g. point density), and forest conditions (e.g. leaf on/leaf off).

Concurrent with the rapid uptake of ALS data for forest inventory assessment has been the growing recognition of the power of long time series optical imagery to provide spatial and historical context to forest dynamics across large spatial and temporal time scales (Frazier et al., 2014; Pflugmacher et al., 2014, 2012; Zald et al., 2016). Specifically, data available from the Landsat series of satellites provides optical multispectral imagery from 1972 to the present. Following the 2008 opening of the United States Geological Survey (USGS) data archive (Wulder et al., 2012), a wide range of data products have become available for analysis (Dwyer et al., 2018). As a result, methodologies and approaches have been developed that allow wide-area characterization of forest cover and change (Hermosilla et al., 2016; Zhu, 2017) facilitated by advances in cloud masking (Zhu and Woodcock, 2014), the generation of surface reflectance products (Masek et al., 2006), and enabled by advanced computing (Wulder and Coops, 2014).

As wall-to-wall estimates of forest attributes are needed for inventory purposes, there is often a need to extrapolate ALS forest attributes across time and space to forests where ALS data has not been acquired. Two-stage sampling approaches have been common in forestry for decades, with attributes such as volume, diameter at breast height (DBH), and height imputed directly from field plots to Landsat data (e.g., Makela and Pekkarinen, 2004; Tomppo et al., 2008). As extensive field data are not often available, incorporating attributes

predicted from ALS data into these imputation approaches is conceptually straightforward and has been successfully undertaken using a number of different approaches. Andersen et al. (2011) incorporated ALS data with Landsat imagery and synthetic aperture radar (SAR) data to improve estimates of biomass across Alaskan boreal forest landscapes. Wilkes et al. (2015) used a two-stage approach combining ALS estimates with multiple satellite datasets and other climate and topographic data to estimate canopy height. Zald et al. (2016) and Matasci et al. (2018a) developed and implemented approaches for imputing forest structure estimates and ALS metrics using Landsat best-available pixel composites in boreal forest conditions for a single year. Matasci et al. (2018b) extended this work to generate estimates of forest structure for the entirety of Canada's forested ecosystems annually, representing over three-decades. The authors found that imputing forest structural attributes on an annual basis enabled the characterization of forest dynamics in disturbed areas as well as trends in forest structure in undisturbed forest stands. Bolton et al. (2018) explored the use of metrics characterizing the full Landsat time series for the imputation of ALS-derived forest structure. These time series metrics included trends in spectral indices (e.g., Tasseled-Cap Transformations (TCT), Normalised Difference Vegetation Index (NDVI), and Normalised Burn ratio (NBR)), as well as time since a detected disturbance event (i.e., as fire or harvest). The authors used samples of area-based estimates of height, basal area, and volume derived using ALS and co-located ground plots for forests in British Columbia, Canada, and found that time series metrics improved imputation results over the use of single-year Landsat metrics (e.g., relative RMSE decreased from 32.1% to 23.3% for basal area when single-year metrics were replaced with 30-year time series predictors).

In this study, we further develop and apply methodologies to estimate forest attributes using Landsat time series data across a number of actively managed forest management areas in Canada covering a variety of forest types, productivities, disturbance regimes, and management strategies, and ask the following questions:

For Landsat time series predictors, is there a time series length that yields the optimum result for forest attribute estimation across a variety of sites and conditions?

Landsat time series metrics can be derived over forest stands for any number of time periods, most often commencing with the availability of Landsat Thematic Mapper data in 1982 (Goward et al., 2006; Wulder et al., 2008), but also in some cases incorporating the entire Landsat record back to 1972 (e.g., Savage et al., 2018). Longer time series will describe more of a forest stand's history, yet will require more data, processing, and storage capacity, while shorter time series will provide a potentially more accurate description of the current forest conditions. Is there an optimum length of time over which to compute spectral trends, and how does the optimum length of time vary between sites that differ in terms of species, productivity, and disturbance history?

Does the inclusion of disturbance information universally improve the accuracy of model predictions or is the benefit of including disturbance information limited to those sites that have frequent disturbances?

Across Canada, multiple forest disturbance regimes exist, and fire in particular varies in frequency, extent, and severity. In Newfoundland, for example, boreal forest ecosystems are infrequently subject to wildfire, with pest, diseases, and harvesting serving as the primary drivers of disturbance history in the province (Arsenault et al., 2016); contrasted with western Canada where large, severe fires are common (White et al., 2017b). Do these differences in disturbance regimes lead to differences in the utility of Landsat time series information for estimating forest attributes? Does historical disturbance information derived from Landsat time series only improve attribute estimation in areas that undergo frequent disturbance?

As more studies demonstrate the predictive gain in accuracy and utility of the wall-to-wall approach through the integration of Landsat time series data and ALS metrics, the development of consistent and

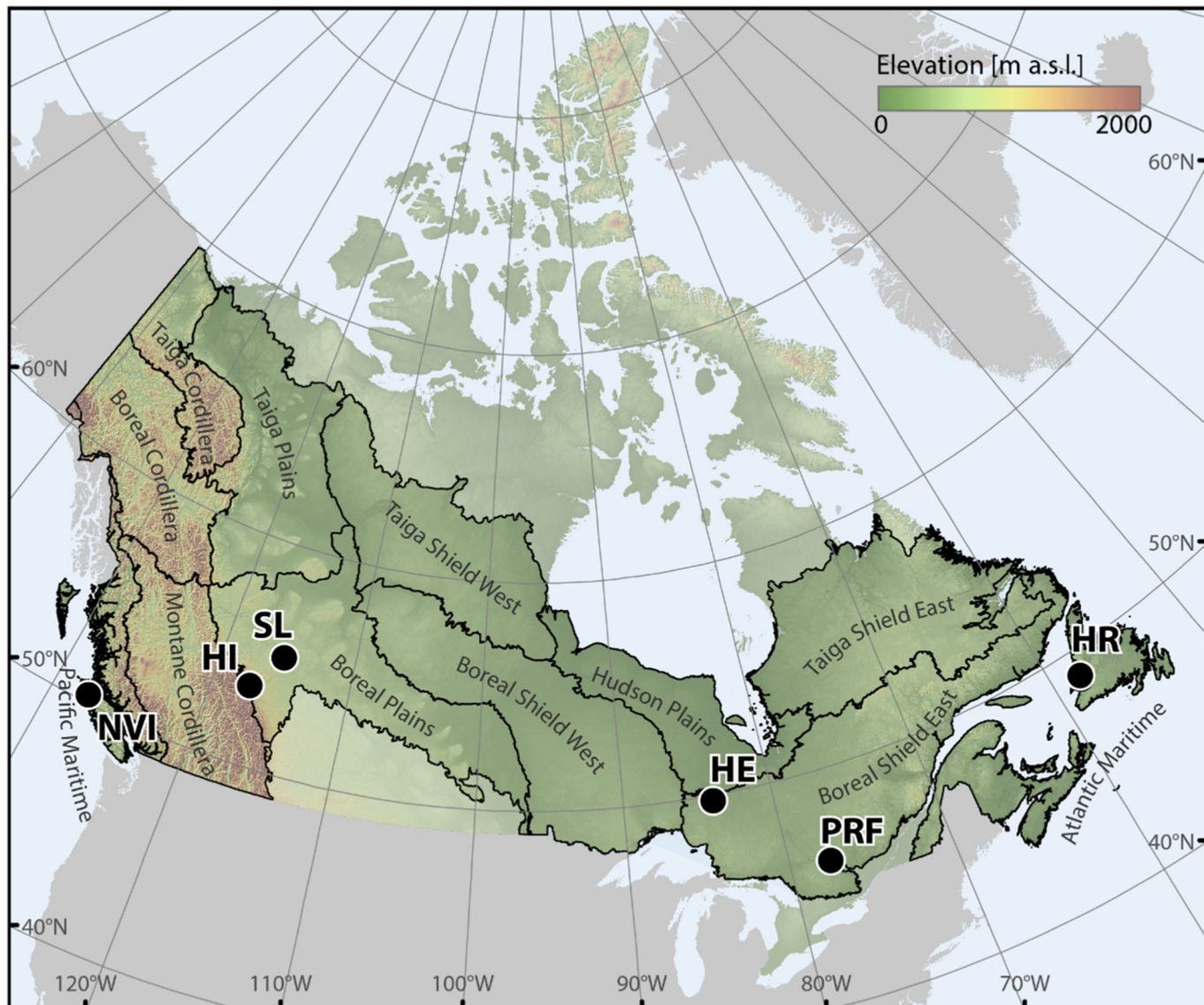


Fig. 1. Location of the six study sites used in the analysis. Harry's River (HR), Hearst (HE), Hinton (HI), North Vancouver Island (NVI), Slave Lake (SL), and Petawawa (PRF). Black polygons depict forested ecozones of Canada.

logical approaches becomes paramount. This study aims to investigate a method for determining which time series information is most critical for forest attribute estimation, leading to the efficient production of relevant wall-to-wall forest attributes, including stand height, basal area, and volume.

2. Methods

2.1. Study area and ALS data description

This study was conducted at six sites located across Canada (Fig. 1) covering a wide range of forest types, terrain conditions, species compositions, stand structural characteristics, and disturbance regimes (described and compared in Table 1). ALS data were available for each of the study sites and were used to generate enhanced forest inventory (EFI) layers (White et al., 2017a; White et al., 2013). EFI layers were generated using an area-based approach. In this approach, predictive models of selected forest attributes were developed using point cloud-derived metrics as predictors. The reference data collected in the field consisted of plot-level summaries of tree-level measurements of diameter-at-breast-height, tree height, and species. The developed EFI

models were then used to estimate forest attributes for the entire area of the point cloud data acquisition at a pixel level. The size of the pixel corresponded to the size of the plot and was equal to 20×20 m for all sites except one (25×25 m for Hinton). Given the nature of using existing EFIs products, we were unable to control the resolution of each individual product.

These EFIs have been operationally developed since early 2000 and were generated independently, with the same general methodology, but varying number of plots, point cloud densities, and modeling approaches (Table 2, Supplementary Table 1). This range in variability in EFIs provides additional opportunity to demonstrate robustness in our approach of how Landsat time series can be used to extrapolate forest inventory attributes.

The wall-to-wall pixel-level estimates included stand height (H), basal area per hectare (BA), and total stem volume per hectare (V) (Table 3, Fig. 2). Measurements of H differed between sites, with Lorry's height measured at Harry's River, North Vancouver Island, Petawawa, and Slave Lake, and top height measured at Hearst and Hinton. Below, we briefly describe each of the study areas, their location and ecozone, ALS point cloud acquisition parameters, available field data, and the EFI modeling. While ALS point densities vary between these

Table 1
Site environmental characteristics for the 6 study sites. Climate data extracted from climate NA (<http://www.climatewina.com/>) (Wang et al., 2016).

Study site	Latitude (N)	Longitude (W)	Annual mean daily temperature (°C)	Average PPT (mm)	Growing degree days (> 5°)	Dominant species	Dominant disturbance agent	Elevation range [m a.s.l.]
Harry's River	48° 46' 22"	58° 11' 44"	3.2	1284	1136	<i>Abies balsamea</i> , <i>Picea mariana</i> , <i>P. glauca</i> , <i>Larix laricina</i> , <i>Harvest, Insect</i>		20–630
Hearst	49° 40' 20"	83° 57' 42"	0.1	794	1234	<i>Betula papyrifera</i> , <i>B. alleghaniensis</i>		35–440
Hinton	53° 23' 8"	117° 11' 20"	1.8	595	983	<i>Picea mariana</i> , <i>P. glauca</i> , <i>Pinus banksiana</i> , <i>Abies balsamea</i> , <i>Populus tremuloides</i>	<i>Harvest, Insect, fire, windthrow</i>	830–2400
North Vancouver Island	50° 17' 28"	127° 24' 1"	6.1	4652	1134	<i>Pinus contorta</i> , <i>Picea mariana</i> , <i>P. glauca</i> , <i>Populus tremuloides</i> , <i>Tsuga heterophylla</i> , <i>Thuja plicata</i> , <i>Pseudotsuga menziesii</i>	<i>Harvest</i>	0–1230
Petawawa Research Forest	45° 58' 54"	77° 29' 45"	4.9	831	1894	<i>Pinus strobus</i> , <i>P. resinosa</i> , <i>Populus tremuloides</i> , <i>Betula papyrifera</i>	<i>Wind, partial harvest</i>	130–282
Slave Lake	55° 0' 52"	115° 22' 57"	1.6	575	1202	<i>Picea glauca</i> , <i>P. mariana</i> , <i>Populus tremuloides</i> , <i>Pinus contorta</i>	<i>Fire, harvest, windthrow</i>	525–1400

datasets, previous research has demonstrated that point density has a minimal impact on the accuracy of forest attribute estimation (Treitz et al., 2012). ALS data acquisition parameters are presented in Table 2 and detailed EFI model results for each site are presented in Supplementary Table 1.

2.1.1. Harry's river, Newfoundland and Labrador (HR)

The Harry's River study region covers 11 km² in the southwest of Newfoundland and contains some of the most productive forests on the island, with a humid continental climate type (Peterson, 2016). ALS data were acquired in 2016 with average point density of 6 points/m². Eighty eight calibration plots were used to develop wall-to-wall EFI estimates of a number of forest stand attributes including H, BA, and V. The models were developed using a random forest (RF) approach with R² values for BA and V highest among all study sites (0.82 and 0.84, respectively), with relative RMSEs of 22.3% and 23.2%, respectively, for BA and V. H had a R² of 0.92 and relative RMSE of 9.6% (Luther et al., 2019).

2.1.2. Hearst, Ontario (HE)

The Hearst site, located in northeastern Ontario, occurs within the terrestrial Boreal Shield Ecozone (Wikren et al., 1996) characterised by flat to rolling terrain, and is actively managed for timber by number of commercial forest companies. The ALS data for Hearst was acquired in 2007 with an average point density of 0.82 points/m². A total of 442 inventory plots were used to develop predictive models using the RF modeling approach (Penner et al., 2013) with RMSEs of 3.6 m²/ha (17%) for BA, 20.26 m³/ha (18%) for V, and 0.71 m (5%) for H.

2.1.3. Hinton, Alberta (HI)

The Hinton study area is located in western Alberta within the Montane Cordillera ecozone characterised by mountainous regions and intermontane valleys. The area is actively managed for timber, but also for other components of the resource sector including oil and gas exploration. ALS data were acquired between 2004 and 2007 with an average point density of 0.75 points/m². A total of 787 inventory plots were used to develop multiple predictive models for BA and V, with R² ranging from 0.73–0.81 for BA models and 0.73–0.90 for V models, while a single model was developed for H (R² = 0.95).

2.1.4. North Vancouver Island, British Columbia (NVI)

The North Vancouver Island study site is located within the Pacific Maritime ecozone characterised by highly fertile environments with mountainous terrain, steep slopes, and large elevation variations. The ALS data for North Vancouver Island was collected in 2012 with average point density of 11.6 points/m². A total of 231 inventory plots were used to develop predictive models for a range of forest stand attributes including H, BA, and V. The most accurate estimations were achieved for H, with R² of 0.94 and relative RMSE of 7.93%. Predictions for BA were of lowest accuracy and had the lowest R² value among all models and all study sites (0.42).

2.1.5. Petawawa Research Forest, Ontario (PRF)

The Petawawa study site is a research forest of the Canadian Forest Service (CFS) and is a mixed mature natural and plantation forest within the Boreal Shield ecozone. The ALS data for Petawawa had a density of approximately 12 points/m². The EFI models were derived based on metrics generated for 85 plots using a RF modeling approach. The model ranged between R² = 0.52 for BA and 0.94 for H. The relative RMSE for BA and V was equal to 25.68% and 30.40%, respectively.

2.1.6. Slave Lake, Alberta (SL)

The Slave Lake site is located in western Alberta within the Boreal Plains ecozone characterised by low land plains with mesic and wetland areas. ALS data was acquired between 2006 and 2008, with the

Table 2
ALS data acquisition parameters.

Study area	Year of acquisition	Sensor	Flying height [m AGL]	Pulse repeat rate	Scanning frequency	Scan angle [+/-]	Average point density
HR	2016	Riegl LMS-Q680i	1000	150Khz	10–200 lines/s	30°	6
HE	2007	Leica ALS50	2400	119 kHz	32 Hz	15°	0.82
HI	2004–2007	Optech ALTM 3100	1400	70 kHz	30–33 Hz	25°	0.75
NVI	2012	ALTM3100EA	700	70 kHz	65 Hz	12.5°	11.6
PRF	2012	Riegl LMS-Q680i	750	150Khz	76.67 Hz	20°	12
SL	2006–2008	Optech ALTM 3100	1250–1400	50–70 kHz	30–33 Hz	25°	1.63

majority acquired in 2008, and an average point density of 1.63 points/m². A total of 98 permanent sample plots were used to develop EFI estimations of H, BA, and V, with R² values ranging from 0.71 for BA to 0.78 for V. Predictions of V had the highest RMSE of 49.19% (Tompalski et al., 2018).

2.2. Data sources

2.2.1. Landsat time series data

Landsat time series predictors and information of disturbance events from 1984 to 2016 were obtained from gap-free Landsat composites, created using the Composite2Change (C2C) method (Hermosilla et al., 2017, 2016). Specifically, summer image composites (August 1 ± 30 days) were created through a best available pixel (BAP) selection process which accounted for distance to clouds, atmospheric contamination, as well as acquisition sensor (see White et al., 2014b for details). Next, noisy observations (e.g., smoke) were removed from the image composites and data gaps were filled through a temporal analysis of spectral trends (Hermosilla et al., 2015a), yielding annual, gap-free image composites across Canada. Disturbances were detected from these image composites (detection accuracy of 89%, Hermosilla et al., 2016) and attributed as harvesting, fire, road, or non-stand-replacing disturbance using spectral, temporal, and geometric information, resulting in an overall attribution accuracy of 92% (Hermosilla et al., 2015b, see Hermosilla et al., 2016 for more information on the C2C product). For this study, four spectral indices were calculated from the annual composites: Tasseled Cap Brightness (TCB), Greenness (TCG), Wetness (TCW), and the normalized burn ratio (NBR) (Crist, 1985; Key and Benson, 2006, 1999).

2.2.2. Topographic data

A 1 arc-second 30 m global digital elevation model (DEM) derived from Advanced Spaceborne Thermal Emission and Reflection Radiometer (ASTER) was obtained for this analysis (Meyer et al., 2011). From the DEM, terrain slope and the topographic solar radiation index (TSRI), a transformed measure of aspect, were derived. TSR was derived as:

$$\text{TSRI} = 0.5 - \cos((\pi/180)(\text{aspect}-30))/2 \quad (1)$$

TSRI ranges from zero (northeast slopes) to one (southwest slopes).

2.3. Building predictive models

To allow for comparisons between EFI estimations and Landsat

spectral data, all EFI datasets were resampled to 30 m using a bilinear interpolation to match the Landsat tessellation. As spatial error in Landsat or ALS data could potentially lead to spatial mismatches between the data sources, all variables were smoothed with a mean filter (3 × 3) from 30 × 30 m to 90 × 90 m before analysis. Additionally, this smoothing step reduced noise in Landsat temporal metrics caused by slight pixel shifts through time. As stands are typically managed at grain sizes larger than 90 × 90 m in Canada, this spatial smoothing can improve estimation accuracy without sacrificing the required spatial detail (Strunk et al., 2014).

To restrict the analysis to forested environments, we removed non-forested areas using annual, national, 30-m land cover maps produced by Hermosilla et al. (2018) from Landsat data. As annual land cover maps were available, information on land cover from the year of each ALS flight was used. To ensure that the full range of structural variability was sampled in the models, the pixels at each study area were stratified into 10 classes based on a k-means clustering of the ALS-derived estimates of H, BA, and V. A stratified random sample of calibration and validation pixels was then selected across the 10 classes, with each class sampled proportionally to the area of the class across the study area. To avoid issues of spatial autocorrelation, a minimum distance of 500 m was set between samples. To avoid sampling pixels that occurred on forest edges, neighboring cells were also required to be forested (i.e., 3 × 3 pixel window). In total, 2000 pixels were randomly sampled from each study area. These samples were divided into a calibration (75%, 1500 samples) and validation (25%, 500 samples) set for each study site. A smaller sample size was used at both North Vancouver Island (1366 pixels) and Petawawa (233 pixels), given the smaller size of these study areas. To obtain 233 sample pixels at Petawawa, the minimum distance between samples was relaxed to 400 m.

2.3.1. Approach for optimizing time series length

Following the selection of sample pixels, Landsat time series predictors were derived for each sample. To determine the optimal time series length for deriving Landsat predictors, the time series length was incrementally increased from one year to the maximum allowable time series length (i.e., 1984 to the year of ALS data collection). At each time series length, three temporal metrics were calculated for TCB, TCG, TCW, and NBR: the median value through time, the interquartile range (IQR) through time, and the Theil Sen slope through time (Jassby and Cloern, 2017; Mann, 1945). In addition to these 12 variables, elevation, terrain slope, and TSR were included in each model, for a total of 15 predictor variables (Table 4). IQR and Theil Sen slope predictors were only included when the time series was > 5 years in length. Models

Table 3

Mean values for ALS-derived estimates of H, BA, and V for each study site. Additionally, the total area of ALS data at each study site is provided. Standard deviations are in parentheses.

Attribute	HR	HE	HI	NVI	PRF	SL
ALS area [× 1000 ha]	112	1537	1156	64	10	658
Landsat area [× 1000 ha]	230	3646	2065	389	17	1013
H [m]	9.0 (2.8)	13.8 (4.9)	18.3 (5.6)	25.5 (10.6)	20.1 (4.6)	20.3 (4.1)
BA [m ² /ha]	21.4 (12.2)	22 (10.4)	27.1 (11.2)	57.3 (31)	23.8 (6.9)	35.4 (10.1)
V [m ³ /ha]	101.8 (74.2)	94.3 (75.4)	143.8 (117.7)	636.3 (451.4)	225.9 (79.3)	271.3 (103.8)

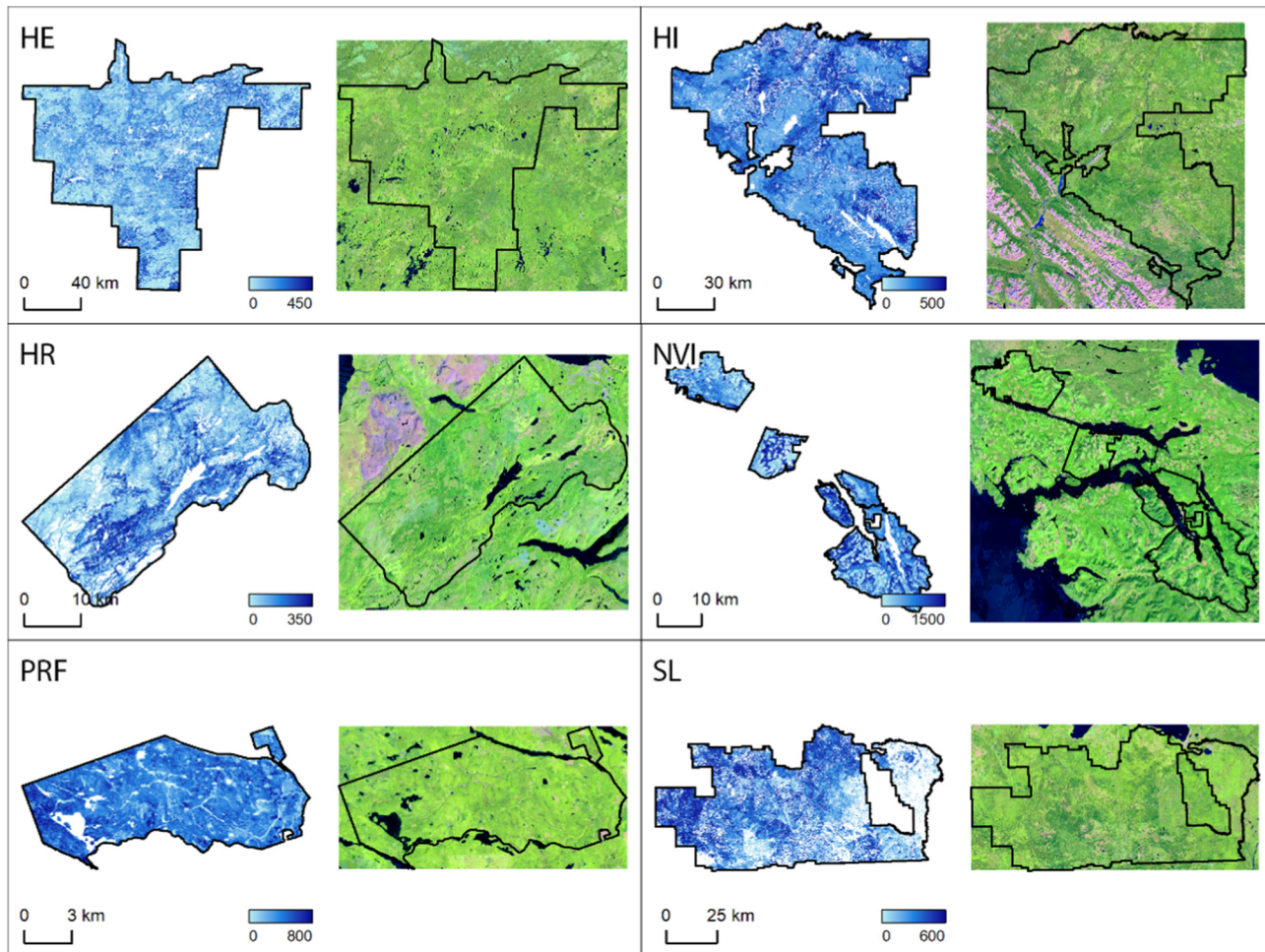


Fig. 2. ALS-derived estimates of stem volume (m^3/ha , left side of each panel), and a Landsat-derived annual image composite (right side of each panel) for each study site (Harrys River (HR), Hearst (HE), Hinton (HI), North Vancouver Island (NVI), Slave Lake (SL), Petawawa (PRF)). Landsat color composites are Band 5/4/3 as R/G/B.

Table 4

Predictor variables used in model development (15 predictor variables in total). Landsat spectral indices include Tasseled Cap Brightness (TCB), Tasseled Cap Greenness (TCG), Tasseled Cap Wetness (TCW), and the Normalized Burn Ration (NBR).

Variable type	Variable	Spectral indices
Topographic	Elevation	-
	Slope	-
	TSRI	-
Landsat time series	Median	TCB, TCG, TCW, NBR
	Interquartile range ^a	TCB, TCG, TCW, NBR
	Theil Sen slope ^a	TCB, TCG, TCW, NBR

^a Only included for models with time series length ≥ 5 years.

were run to predict H, BA, and V using random forest (RF) regression, resulting in up to 33 models for each study site (i.e., 33 time series lengths). Specifically, the randomForest package in R was used to develop each model using 500 regression trees (Breiman, 2001; Liaw and Wiener, 2002; R-Core-Team, 2013). Using the 500 validation samples, model accuracy was evaluated using the coefficient of determination (R^2), the root mean squared error (RMSE), as well as the model bias:

$$\text{RMSE} = \sqrt{\frac{1}{n} \sum_{i=1}^n (\text{Predicted}_i - \text{Observed}_i)^2} \quad (2)$$

$$\text{Bias} = \frac{1}{n} \sum_{i=1}^n (\text{Predicted}_i - \text{Observed}_i) \quad (3)$$

where Predicted_i is the modeled value for the i th sample and Observed_i is the ALS-derived estimate. In addition, relative RMSE and bias (RMSE%, bias%) were derived relative to the mean of the ALS-derived estimates at each study area. Through an investigation of the relationships between R^2 , RMSE, bias and time series length, the optimal time series length could be explored at each study site.

To determine if information on disturbance history could improve model performance, a second set of models was run that included Landsat derived information on disturbance as predictors in addition to the predictors in Table 4. Two variables to describe disturbances were included using the C2C disturbance product presented in Section 2.2.1: disturbance type and time since disturbance. Disturbance type was labelled as either stand replacing (i.e., fire, harvest, road) or non-stand replacing. If no disturbance was recorded for a pixel, years since disturbance was set to 50 years, following the approach of Matasci et al. (2018a).

3. Results

3.1. Time series length

Fig. 3 displays model results (R^2 , RMSE%, bias%) as a function of the time series length used to calculate Landsat predictor variables. R^2

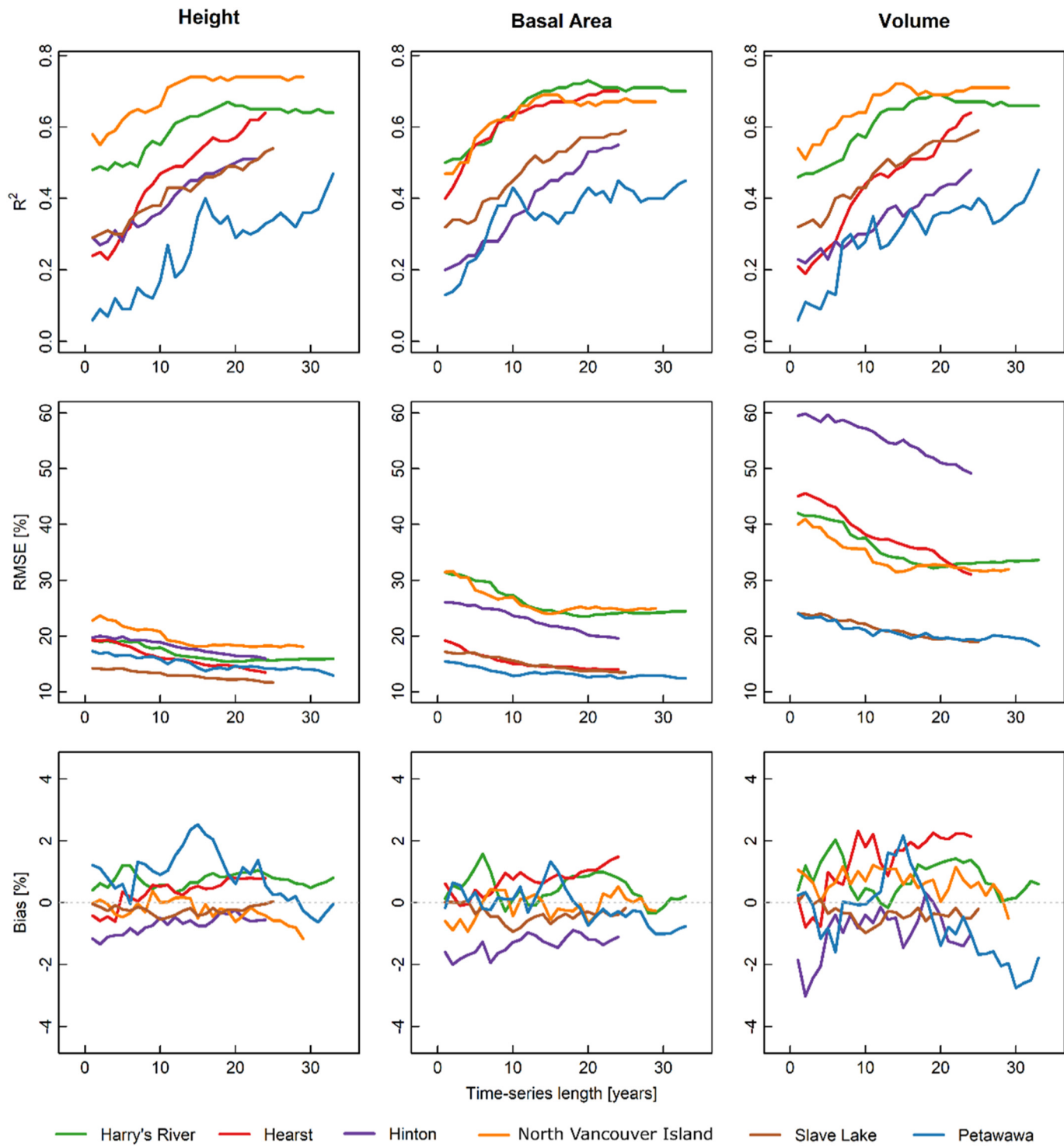


Fig. 3. R^2 , RMSE, and Bias for attribute estimates as a function of the time series length for the predictor variables. Note R^2 starts at 0.0 while RMSE(%) starts at 10%.

values were similar between H, BA and V models, with the peak R^2 ranging from 0.47–0.74 for H, 0.45–0.73 for BA, and 0.48–0.72 for V. R^2 values were typically highest for Harry's River (peak $R^2 = 0.67\text{--}0.73$) and North Vancouver Island (peak $R^2 = 0.69\text{--}0.74$), and lowest for Petawawa (peak $R^2 = 0.45\text{--}0.48$). In general, R^2 values at each site tended to increase as the time series got longer. While R^2 tended to plateau for Harry's River and North Vancouver Island around 15 years, R^2 continued to increase for Hearst, Slave Lake, and Hinton until the maximum time series length was reached (24–25 years). For example, when the time series length was increased from 5 to 24 years,

the R^2 for H increased from 0.30 to 0.64 at Hearst, 0.30 to 0.53 at Slave Lake, and 0.28 to 0.53 at Hinton. For BA, the R^2 increased from 0.55 to 0.70 at Hearst, 0.34 to 0.58 at Slave Lake, and 0.24 to 0.55 at Hinton. Similarly increases in R^2 were observed for V (0.26 to 0.64 at Hearst, 0.35 to 0.58 at Slave Lake, and 0.23 to 0.48 at Hinton). While results for Petawawa were noisier, likely due to the small sample size, similar increasing trends were also observed.

RMSE% was lowest for H models (minimum RMSE% = 11.6–18.0), followed by BA (minimum RMSE% = 13.5–23.5), and highest for V (minimum RMSE% = 18.2–49.2). Large differences in RMSE% existed

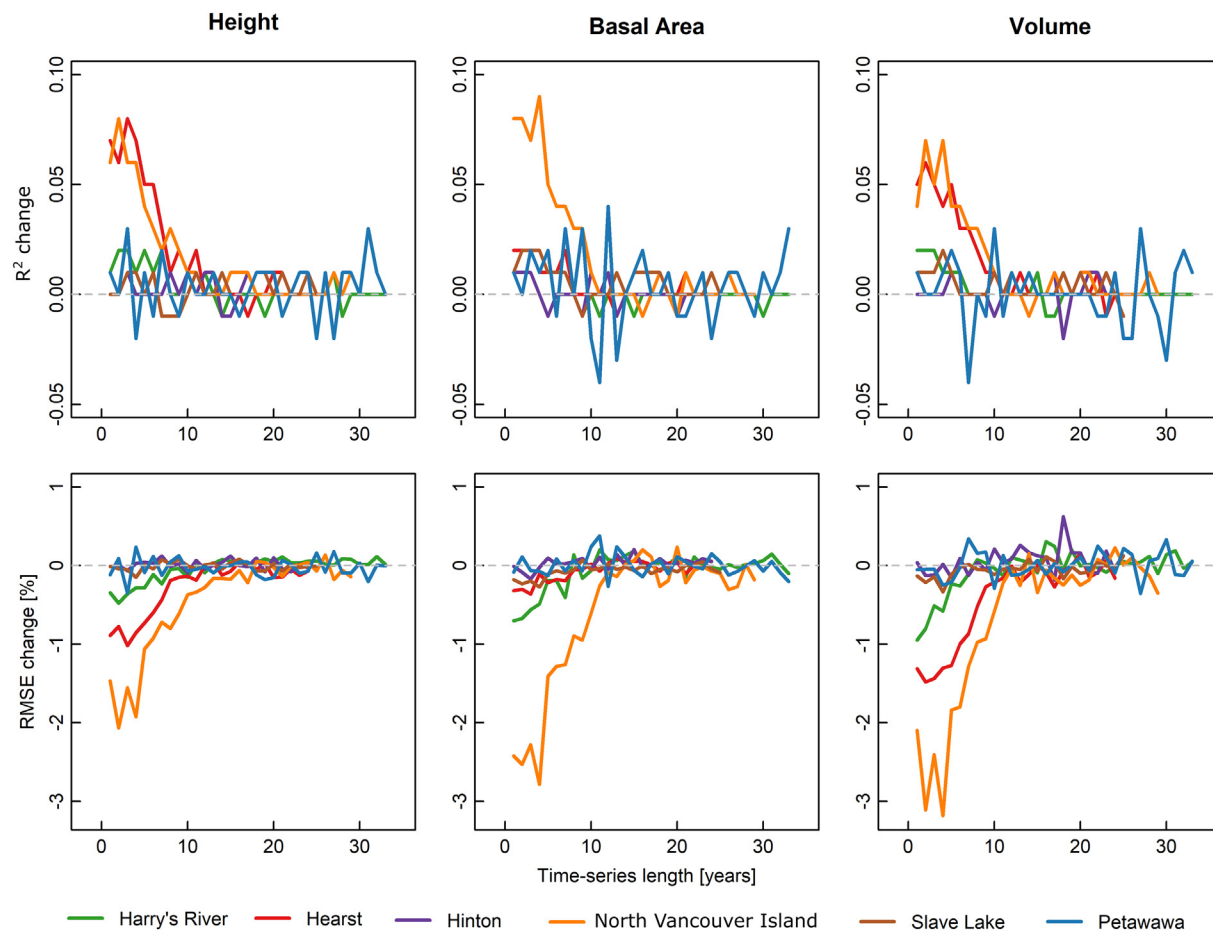


Fig. 4. Change in R^2 and RMSE at each time-step if two additional predictor variables are added to the model: time since last disturbance and disturbance type. The addition of these variables improves models when the time series is short at several sites (R^2 increases, RMSE decreases), but not once the time series is > 10 years in length.

between sites for V, with RMSE% highest in Hinton (minimum RMSE% = 49.2), and lowest in Petawawa and Slave Lake (minimum RMSE% = 18.2 and 18.9, respectively). RMSE% tended to show a gradual decrease as time series length increased. The majority of models had bias values between $\pm 2\%$, and no consistent trends were observed for bias as time series length increased across sites. Hearst and Petawawa did experience a directional change in bias as the time series lengthened for V estimates, with an increasing positive bias for Hearst and increasing negative bias for Petawawa as the time series lengthened.

3.2. Landsat-derived disturbance

Fig. 4 displays the change in R^2 and RMSE at each time-step when time since last disturbance and disturbance type are added as predictors to the models. At Hearst and North Vancouver Island, the addition of these variables improved the models when the time series was short (i.e., R^2 increases, RMSE decreases), but these variables have a minimum effect once the time series is > 10 years in length. For the rest of the sites, the addition of change information was negligible at all time series lengths. Of the selected calibration and validation pixels, North Vancouver Island and Harry's River included the most samples that experienced change during the Landsat record according to the C2C disturbance product (16.2 and 14.5% for North Vancouver Island and Harry's River, respectively, Table 5). At North Vancouver Island, most of this disturbance was harvesting (12.3% of the samples), while at Harry's River, the dominant disturbance was non-stand replacing (7.6%) followed by harvesting (5.7%).

Table 5

Percentage of calibration/validation pixels that experienced change during the Landsat record. Disturbance type determined from C2C Landsat disturbance information.

Site	% disturbed	% burned	% harvested	% non-stand replacing
HR	14.5	0.6	5.7	7.6
HE	9.5	0.1	7.1	2
HI	7.5	0.1	5.9	1
NVI	16.2	0.2	12.3	3.1
SL	11.5	2.6	7	1.4
PRF	3.4	0	1.3	1.7

3.3. Variable importance

Fig. 5 displays how often each variable was an important predictor across 18 models (6 sites \times 3 forest attributes), using variable importance scores from RF. For each site, only the model using the maximum time series length was included. The median and Thiel Sen slope classes of predictors were typically more important than the interquartile range predictors. In terms of spectral indices, NBR and TCW were typically more important than TCB and TCG. NBR was the most important spectral index, with median NBR being the most important predictor variable in 56% of the models, and one of the top two predictor variables in 72% of models. Elevation was the most important terrain variable (in the top two in 44% of models), while TSRI was not a top predictor in any models. Supplementary Figs. 3, 4, and 5 provide the full variable importance scores for each study site.

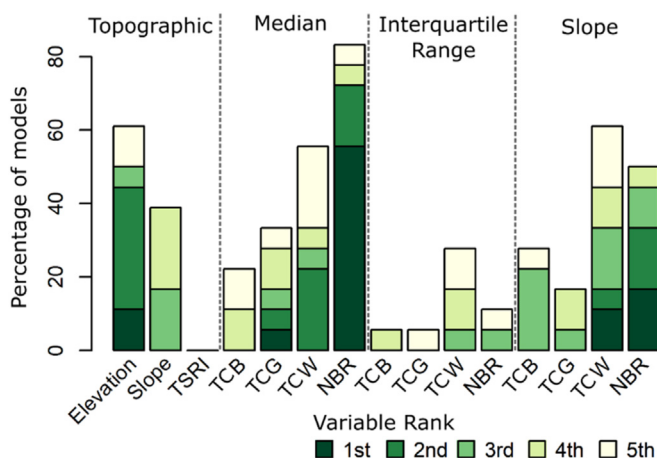


Fig. 5. Percentage of models in which each variable was in the top-five most important variables.

Scatterplots of observed basal area (ALS-derived estimates) against predicted basal area for held-out samples reveal strong correspondences across sites (Fig. 6, H and V results are presented in supplementary material). The narrow range of observed basal area and small sample size at Petawawa contribute to the lower correlations observed. Mapped results of ALS-derived H and predicted H in Fig. 7 reveal the spatial correspondence between ALS and Landsat derived estimates of forest structure.

4. Discussion

Landsat time series data is a valuable source of information for extrapolating estimates of forest attributes derived from ALS data both

spatially and temporally, and improves upon models that only use a single year of Landsat data, or short time series, to make attribute estimations (Bolton et al., 2018; Pflugmacher et al., 2014). While Bolton et al. (2018) demonstrated that longer time series of Landsat data were best for a managed interior forest area in British Columbia, this study has demonstrated that increasing the time series length leads to improved models across a range of forest types, productivities, and disturbance histories across Canada.

We found that there was not a universal optimal time series length that was common to all six study sites. The improvement when the time series length was increased was small in certain locations (Harry's River, North Vancouver Island) and large in others (Hinton, Slave Lake, Hearst, Petawawa). As the prediction accuracy was greatest at Harry's River and Northern Vancouver Island, the plateau of model accuracy at ~15 years suggests that there may be a limit to the improvements that can be gained by maximizing time series length. Bolton et al. (2018) found that maximizing the length of the available time series offered the greatest benefit in terms of improving model estimates. Herein, we found that this effect is not universal across our six study locations. In context, the use of a shorter time series could be beneficial, as more historical estimates of structure can be made. For example, a model that requires only five years of Landsat data could produce estimates of structure annually from 1988-present, while a model that requires 30 years of Landsat data could only produce estimates from 2013 to the present (assuming a time series that starts in 1984). Therefore, the optimal time series length will vary depending on the attribute being modeled, the application, and the relationship between model accuracy and time series length. Specifically, applications that require information on change in forest structure through time may benefit from choosing the shortest possible time series length that meets the accuracy requirements, as short time series will allow for historical estimates over the study area. Alternatively, if the goal is to derive the most accurate estimates of current conditions, the time series length that

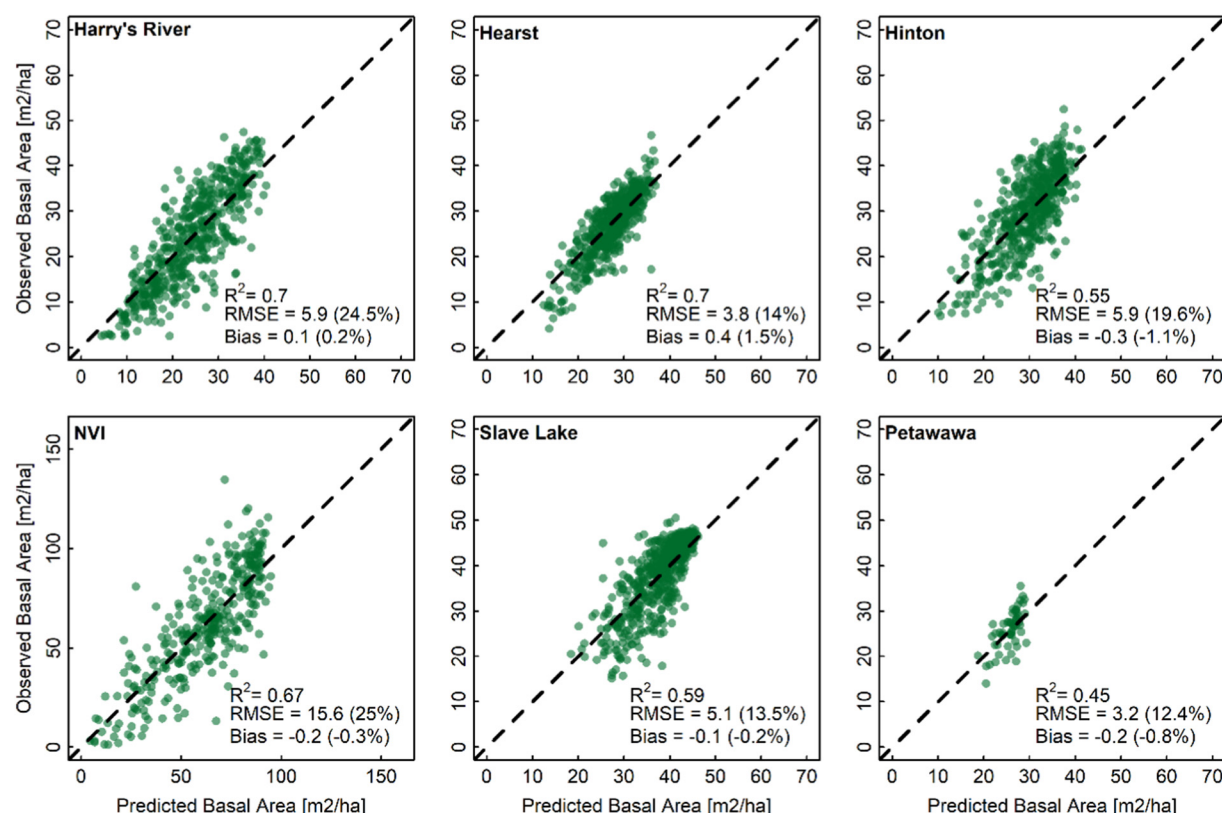


Fig. 6. Scatterplots between observed and predicted basal area at each study site for 500 independent samples. The displayed model uses the longest possible time series of Landsat data at each site. Scatterplots for stand height and volume are included in the supplementary material (Supplementary Figures 1 and 2).

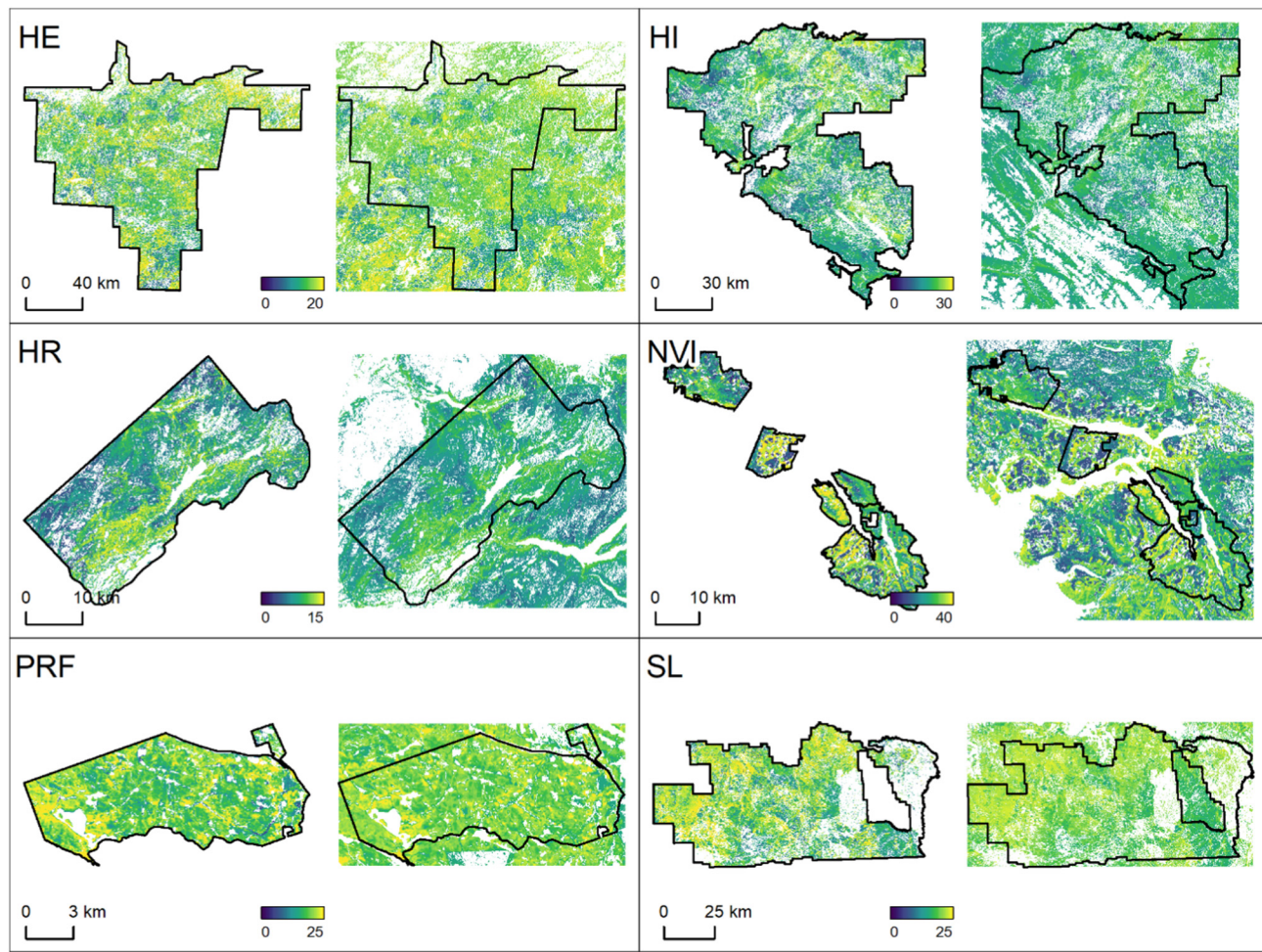


Fig. 7. Side by side maps of height estimates (in meters) derived from ALS (left) vs Landsat (right) at each study site.

produces the highest accuracies can be chosen.

Across the majority of sites and variables, model accuracy, as assessed by R^2 , tended to plateau with increasing time series length around an R^2 of 0.6–0.75. At sites where model accuracy did not plateau with increasing time series length (e.g., Slave Lake and Hinton), the maximum R^2 tended to remain below this apparent “ceiling” of model accuracy, suggesting that these particular models may continue to improve with increasing time series length until this ceiling of model accuracy is reached. Further, while not observed here, we anticipate that model accuracy would eventually decrease with longer time series after the plateau is reached when models are built using the proposed set of predictor variables. Specifically, as more years are incorporated in the calculation of spectral means and measures of temporal variability, these summary statistics may no longer accurately describe current forest structure conditions. To address this, future analyses could benefit from incorporating both short and long term spectral summaries, as short-term metrics may provide insight to current conditions, while long-term metrics provide historical context. The observed “ceiling” of model accuracy may also represent an inherent limitation of optical remote sensing for predicting vertical forest structure, at least with the set of predictor variables we proposed, and further improvements in accuracy may be dependent on data fusion with other remote sensing data sources (e.g., ALS, RADAR).

Spectral indices that utilize mid-infrared reflectance (NBR and TCW) were consistently the most important predictors of structural attributes, which is in agreement with existing studies (Bolton et al., 2018; Cohen and Spies, 1992; Wilkes et al., 2015; Zald et al., 2016). For example, Cohen and Spies (1992) found TCW to be the most sensitive

tasseled cap component to variability in forest structural attributes in Oregon and Washington, while TCW was the most important spectral index for predicting structural attributes in Canadian studies (Bolton et al., 2018; Zald et al., 2016) as well as in New Zealand (Wilkes et al., 2015). Our finding that NBR was the most important spectral index suggests that additional information from the mid-infrared channels can be gained in addition to TCW (Cohen et al., 2018). Cohen et al. (2018) published a Disturbance Signal to Noise Ratio (DSNR) metric and reported that the SWIR bands (and indices based on the SWIR) had the highest median DSNR values.

Both the median spectral conditions and the Theil Sen slope of spectral indices through time were important predictors of structure. A positive slope through time for TCW or NBR could indicate stand development following a disturbance that occurred prior to the start of the time series. Therefore, while a young forest may resemble a mature forest spectrally once canopy closure is reached, the slope of spectral indices through time may provide insight to the age and development of the stand. The finding that the interquartile range was rarely important suggests that the most meaningful information on spectral variability is captured by the slope of the TCW or NBR spectral trend.

For our second research question, we did not find that the inclusion of disturbance information markedly improved model outcomes, and we found no substantive difference with their inclusion between sites that were disturbed more frequently versus those sites that were disturbed less frequently. Directly incorporating information on disturbance history (i.e., time since last disturbance and type of disturbance) should improve model accuracies when long time series are used. However, because few samples in this analysis were disturbed

during the Landsat record (Table 5), we did not see the added benefit of disturbance information. This result is similar to that of Bolton et al. (2018), who found that including information on disturbance did not lead to improved model outcomes. The number of disturbed samples was low in this analysis because the majority of areas disturbed during the Landsat record had not yet returned to a forested state by the time of ALS collection, and therefore EFI estimates were not produced for these pixels. If recently disturbed stands had been included, disturbance variables would likely have had greater importance in the models, and should therefore continue to be considered in future analyses.

The ability to estimate highly accurate plot level forest structure attributes such as H, V and BA over larger areas has always been a necessity and goal of forest inventory approaches. In the approach developed in this paper, the detailed inventory attribute estimates that are generated using an area-based approach with co-located ALS and ground plot data can be extended over larger areas, further leveraging investments in ALS data to the benefit of surrounding forest areas. As a result, the approach presented herein provides the opportunity to extend EFIs across larger areas, providing regional characterizations of structure in areas where the full cost of a conventional inventory cannot be justified. There are however some important caveats. ALS data and resulting EFIs often target areas with high-value commercial species in the most productive forests. As such, they represent a biased sample from which to extrapolate basic forest inventory attributes to lower productivity, unmanaged forest areas. Additionally, while information on tree species is often required for management decisions, most EFIs do not provide species composition, and species identification is difficult with the spectral and spatial resolution of Landsat data. Therefore, the approach presented in this analysis is not intended as a replacement for species-specific inventory data, but rather a means to extend highly accurate estimates of forest inventory attributes (as captured in an EFI) to managed forests that lack EFI (either as a function of disturbance or inventory vintage) as well as unmanaged forest areas or areas that currently lack inventory information. While Landsat-derived estimates of forest attributes are not sufficient to replace inventory data, these data are invaluable for monitoring regional and national trends and for supporting modeling needs (e.g., carbon modeling, habitat characterization). A known limitation of assessing forest structure with optical remote sensing is the saturation effect that occurs for vegetation indices at high levels of biomass in dense, closed forest canopies (Goetz and Dubayah, 2011). While using a long time-series of observations helps address this issue, as done here, the saturation effect may still be present in stands that were dense and closed for the entirety of the time-series, leading to underestimation of H, BA, and V at high values for certain sites (Fig. 6, and Supplementary Figs. 1 and 2). This finding further exemplifies why the proposed approach is intended to complement, and not replace, EFIs.

What also must be considered is the level of error and uncertainty associated with the original EFI estimates. Herein, our interpretation of the relative advantages of time series length assumes a uniform level of uncertainty in the original EFI estimates, which are then estimated using the Landsat time series and ancillary predictors. In reality, those EFI models have different levels of uncertainty associated with them that in turn can impact their extrapolation across the landscape. For example, in Hinton, we know that the calibration data did not represent the full range of forest structure conditions found (disproportionately representing younger, shorter stands) within the forest management area and that deciduous and mixed conditions were poorly represented (White et al., 2014a). This lack of representation poses particular challenges for RF, the modeling approach used to generate the EFI outputs in Hinton. There was also a time lag between ground plot and ALS data collection that was variable, and the plots were not of a uniform size, nor did they exactly match the extent of the ALS grid cell. Further, the EFIs in this study were produced using different modeling approaches and point densities. We believe this to be a strength rather than a weakness of the study, as these data exemplify the range of EFIs

produced across Canada for the past 15 years and provide a representative sample upon which to demonstrate how Landsat time series can be used across a range of forest conditions and EFI approaches. To clarify, our aim is not to explicitly include Landsat time series data in the production of the EFI itself. Rather by using the published EFIs, we have ensured that inventories were developed in a scientifically robust and transparent manner, availing upon best practices as documented in the scientific literature. As such, the underlying accuracy of the EFIs used in our analysis is not as important to the objectives of our study as the trends in attributional accuracy with varying time series length.

Additionally, two-phase modeling approaches used to estimate forest stand attributes over large areas may be associated with complex statistical challenges to properly account for the uncertainty in the two modeling steps. Saarela et al. (2016) demonstrated that when the uncertainty of the intermediate ALS model is ignored, which was the case in the majority of existing studies, the estimated variance of the estimator can be biased (underestimated). They proposed a model-based estimator that takes into account both the uncertainty associated with the intermediate ALS model, and the final model based on the predictors derived from satellite images. However, the proposed approach requires ordinary least squares regression models to be used during both modeling steps. To the best of our knowledge, an estimator for the prediction variance when using non-parametric approaches and two-phase modeling is not yet derived. While error must be considered at both modeling steps (ground to ALS and ALS to satellite imagery), it is important to stress that our study focused on the second modeling step only (ALS to satellite imagery), with the goal of improving our understanding of the approaches that lead to the most accurate extrapolation of ALS-derived estimates.

It did not appear that model accuracies in this analysis were directly related to the underlying accuracies of the EFIs used as inputs. For example, Hinton had some of the highest accuracies for the EFI (Supplementary Table 1), but some of the weaker models between the EFI and Landsat time series data. We suspect that underlying characteristics of the ALS data, and the structural complexity of the study sites are more important determinants of the accuracy of our models than the underlying accuracy of the EFIs. For example, the ALS data for Hinton was collected over a four year period (2004–2007), meaning that the EFI does not represent one consistent time period, leading to a temporal mismatch with the Landsat time series data. Model accuracies were typically lowest at Petawawa, which may have been caused by the relatively low number of calibration/validation samples at this site. However, the accuracies at Petawawa could have also been influenced by management practices and the diversity of tree species that exist at the site. Petawawa is managed under partial harvesting systems, which may contribute to uncertainties in both EFI estimates as well as subsequent estimates with Landsat time series data. For example, partial harvests may not be detected as stand replacing disturbance events with Landsat, preventing time since disturbance from informing model estimates. Additionally, if partially harvested stands are not adequately sampled in model development, the unique spectral trends of partial harvested stands may not be captured in the model. Therefore, partially harvested stands may represent a unique challenge for estimating forest structure with Landsat time series, and should be investigated further. In addition to management practices, Petawawa is also the most diverse of the six study sites, consisting of a mixed forest type of 14 tree species.

The free and open access to the Landsat satellite archive, and similar availability of more recent Sentinel-2 data (Drusch et al., 2012), has enabled the development of national and global initiatives to monitor and report land cover change and dynamics. As a result, new methods and approaches exist to exploit these rich data holdings, offering insights into the future of big geographic data processing and routine production of spatially extensive, yet fine grained, forest information products. The approach demonstrated in this paper fuses these two complementary information sources: time series of medium resolution

surface-reflectance image composites covering each of the study sites, and EFI estimates generated using an area-based approach with co-located samples of airborne ALS and ground plot data. By combining these two remotely sensed data sources, the three-dimensional information provided by ALS and the extensive spatial and temporal coverage of satellite imagery can be fully exploited (Matasci et al., 2018a, 2018b).

The results presented in this paper also highlight the added benefit of using time series rather than a single-date image for the estimation of forest structure. Improvements in Landsat data availability and processing routines have yielded significant methodological improvements for extraction of land cover and biophysical attributes using image time series (Gómez et al., 2016; Hermosilla et al., 2018; Wulder et al., 2018), providing previously unavailable information on forest dynamics at a range of temporal scales (Kennedy et al., 2012; Hansen et al., 2013). Research across Canada (e.g., Hermosilla et al., 2015b) confirms that examining a spectral trajectory derived from Landsat time series enables detection of both non-stand replacing and stand-replacing changes, while bi-annual comparisons only allow us to detect major changes. This is particularly important as forest ecosystems are highly dynamic and many processes, including growth, disturbance, and fragmentation, are processes rather than single events (Hermosilla et al., 2019). This may become even more important as forests respond to environmental change (i.e., climate change and the associated impacts on biodiversity, productivity, disease, insect infestations, etc.).

5. Conclusions

Consistent with prior studies, our study demonstrates value in combining ALS with Landsat time series data to extrapolate estimates of forest attributes. Uniquely, we have applied a consistent methodology across six different locations with different forest conditions and management histories. Longer time series of Landsat data (> 15 years) consistently produced more accurate estimates of forest structural attributes than short time series across a range of forest types, productivities, and disturbance histories. While our results suggest that a single optimal time series length does not exist, we have developed an approach that can be used to determine the optimal time series length on a case by case basis. The optimal time series length will vary depending on application, as applications that require historical estimates must be based on short time series inputs (i.e., allows models to be transferred further back in time). The addition of Landsat-derived information on disturbance history did not improve model performance in this study, as only a small percentage of the sampled pixels experienced change during the Landsat record, due to the fact that most recently disturbed stands did not have attribute predictions in the EFIs. Future studies should explicitly include recently disturbed sites to assess the utility of disturbance information. While decreases in model accuracies were not observed as the time series lengthened, we would expect accuracies to eventually decrease with longer time series data with the set of predictor variables used in this study, as spectral means and measures of variability calculated over long time periods will not always accurately describe current forest conditions, especially in landscapes undergoing frequent disturbance. With the development of this methodological approach, which we have demonstrated across sites, we aim to simplify methods to capitalise on the volume of remotely sensed data, which has grown immensely in recent years (Ma et al., 2015). The method is designed to predict a number of forest attributes, and demonstrate the applicability over a number of forested sites across Canada.

Author contribution statement

Bolton, Coops, White, and Wulder developed the ideas and concepts for this paper. Bolton performed the analysis, prepared the figures, and led the paper writing. Tompalski provided critical support in gathering,

developing, and using the EFIs, along with writing and figure preparation support. Hermosilla provided the Landsat time series data, provided support for using the data, and assisted in writing. Coops, White, and Wulder also provided substantial writing assistance. Queinnec provided input and coding for the modeling approach. Luther, van Lier, Fournier, Woods, Treitz, van Ewijk, Graham, and Quist provided EFI input layers for the analysis, critical insights to interpreting these datasets, and interpretations of the modeling results.

Declaration of competing interest

The authors declare that they have no known competing financial interests or personal relationships that could have appeared to influence the work reported in this paper.

Acknowledgements

This study was funded by the AWARE (Assessment of Wood Attributes using Remote sEning) Natural Sciences and Engineering Research Council of Canada Collaborative Research and Development grant to a team led by Dr. Nicholas Coops (CRDPJ 462973-14). Additionally, we would like to thank Kyle Rosychuk of West Fraser for feedback and insights during the writing of this manuscript.

Appendix A. Supplementary material

Supplementary tables and figures for this article can be found online at <https://doi.org/10.1016/j.rse.2020.111645>.

References

- Andersen, H.E., Strunk, J., Temesgen, H., Atwood, D., Winterberger, K., 2011. Using multilevel remote sensing and ground data to estimate forest biomass resources in remote regions: a case study in the boreal forests of interior Alaska. *Can. J. Remote. Sens.* 37, 596–611. <https://doi.org/10.5589/m12-003>.
- Arsenault, A., LeBlanc, R., Earle, E., Brooks, D., Clarke, B., Lavigne, D., Royer, L., 2016. Unravelling the past to manage Newfoundland's forests for the future. *For. Chron.* 92, 487–502. <https://doi.org/10.5558/tfc2016-085>.
- Bolton, D.K., White, J.C., Wulder, M.A., Coops, N.C., Hermosilla, T., Yuan, X., 2018. Updating stand-level forest inventories using airborne laser scanning and Landsat time series data. *Int. J. Appl. Earth Obs. Geoinf.* 66, 174–183. <https://doi.org/10.1016/j.jag.2017.11.016>.
- Breiman, L., 2001. Random forests. *Mach. Learning* 45, 5–32.
- Cohen, W.B., Spies, T.A., 1992. Estimating structural attributes of Douglas-fir/western hemlock forest stands from landsat and SPOT imagery. *Remote Sens. Environ.* 41, 1–17. [https://doi.org/10.1016/0034-4257\(92\)90056-P](https://doi.org/10.1016/0034-4257(92)90056-P).
- Cohen, W.B., Yang, Z., Healey, S.P., Kennedy, R.E., Gorelick, N., 2018. A LandTrendr multispectral ensemble for forest disturbance detection. *Remote Sens. Environ.* 205, 131–140. <https://doi.org/10.1016/j.rse.2017.11.015>.
- Coops, N.C., Tompalski, P., Nijland, W., Rickbeil, G.J.M., Nielsen, S.E., Bater, C.W., Stadt, J.J., 2016. A forest structure habitat index based on airborne laser scanning data. *Ecol. Indic.* 67, 346–357. <https://doi.org/10.1016/j.ecolind.2016.02.057>.
- Crist, E.P., 1985. A TM tasseled cap equivalent transformation for reflectance factor data. *Remote Sens. Environ.* 17, 301–306.
- Drusch, M., Del Bello, U., Carlier, S., Colin, O., Fernandez, V., Gascon, F., Hoersch, B., Isola, C., Laberinti, P., Martimort, P., Meygret, A., 2012. Sentinel-2: ESA's optical high-resolution mission for GMES operational services. *Remote Sens. Environ.* 120, 25–36. <https://doi.org/10.1016/j.rse.2011.11.026>.
- Dwyer, J.L., Roy, D.P., Sauer, B., Jenkerson, C.B., Zhang, H.K., Lymburner, L., 2018. Analysis ready data: enabling analysis of the landsat archive. *Remote Sens.* 10. <https://doi.org/10.3390/rs10091363>.
- Frazier, R.J., Coops, N.C., Wulder, M., Kennedy, R., 2014. Characterization of above-ground biomass in an unmanaged boreal forest using Landsat temporal segmentation metrics. *ISPRS J. Photogramm. Remote Sens.* 92, 137–146. <https://doi.org/10.1016/j.isprsjprs.2014.03.003>.
- Goetz, S., Dubayah, R., 2011. Advances in remote sensing technology and implications for measuring and monitoring forest carbon stocks and change. *Carbon Manag* 2, 231–244. <https://doi.org/10.4155/cmt.11.18>.
- Gómez, C., White, J.C., Wulder, M.A., 2016. Optical remotely sensed time series data for land cover classification: a review. *ISPRS J. Photogramm. Remote Sens.* 116, 55–72. <https://doi.org/10.1016/j.isprsjprs.2016.03.008>.
- Goward, S.N., Arvidson, T.J., Williams, D.L., Faundeen, J., Irons, J., Franks, S., 2006. Historical record of Landsat global coverage: mission operations, NSLRSDA, and international cooperators stations. *Photogramm. Eng. Remote Sens.* 72, 710–720.
- Hansen, M.C., Potapov, P.V., Moore, R., Hancher, M., Turubanova, S.A.A., Tyukavina, A., Thau, D., Stehman, S.V., Goetz, S.J., Loveland, T.R., Kommareddy, A., 2013. High-resolution global maps of 21st-century forest cover change. *science.* 342 (6160), 850–853.
- Hermosilla, T., Wulder, M., White, J.C., Coops, N., Hobart, G.W., 2015a. An integrated

- Landsat time series protocol for change detection and generation of annual gap-free surface reflectance composites. *Remote Sens. Environ.* 158, 220–234. <https://doi.org/10.1016/j.rse.2014.11.005>.
- Hermosilla, T., Wulder, M.A., White, J.C., Coops, N.C., Hobart, G.W., 2015b. Regional detection, characterization, and attribution of annual forest change from 1984 to 2012 using Landsat-derived time-series metrics. *Remote Sens. Environ.* 170, 121–132. <https://doi.org/10.1016/j.rse.2015.09.004>.
- Hermosilla, T., Wulder, M.A., White, J.C., Coops, N.C., Hobart, G.W., Campbell, L.B., 2016. Mass data processing of time series Landsat imagery: pixels to data products for forest monitoring. *Int. J. Digit. Earth* 9, 1035–1054. <https://doi.org/10.1080/17538947.2016.1187673>.
- Hermosilla, T., Wulder, M.A., White, J.C., Coops, N.C., Hobart, G.W., 2017. Updating Landsat time series of surface-reflectance composites and forest change products with new observations. *Int. J. Appl. Earth Obs. Geoinf.* 63, 104–111. <https://doi.org/10.1016/j.jag.2017.07.013>.
- Hermosilla, T., Wulder, M.A., White, J.C., Coops, N.C., Hobart, G.W., 2018. Disturbance-informed annual land cover classification maps of Canada's forested ecosystems for a 29-year Landsat time series. *Can. J. Remote. Sens.* 44, 1–21. <https://doi.org/10.1080/07038992.2018.1437719>.
- Hermosilla, T., Wulder, M.A., White, J.C., Coops, N.C., Pickell, P.D., Bolton, D.K., 2019. Impact of time on interpretations of forest fragmentation: three-decades of fragmentation dynamics over Canada. *Remote Sens. Environ.* 222, 65–77. <https://doi.org/10.1016/j.rse.2018.12.027>.
- Jassby, J.E., Cloern, A.D., 2017. Wq: Some Tools for Exploring Water Quality Monitoring Data. R Package Version 0.4.9.
- Kangas, A., Maltamo, M. (Eds.), 2006. Forest Inventory: Methodology and Applications. Springer, Netherlands. [https://doi.org/10.1016/0031-8663\(66\)90016-0](https://doi.org/10.1016/0031-8663(66)90016-0).
- Kennedy, R.E., Yang, Z., Cohen, W.B., Pfaff, E., Braaten, J., Nelson, P., 2012. Spatial and temporal patterns of forest disturbance and regrowth within the area of the Northwest Forest Plan. *Remote Sens. Environ.* 122, 117–133. <https://doi.org/10.1016/j.rse.2011.09.024>.
- Key, C.H., Benson, N.C., 1999. Measuring and remote sensing of burn severity: the CBI and NBR. In: Proceedings Joint Fire Science Conference and Workshop, pp. 284.
- Key, C.H., Benson, N.C., 2006. Landscape Assessment: Sampling and Analysis Methods. USDA For. Serv. Gen. Tech. Rep. RMRS-GTR-164-CD. pp. 1–55.
- Leckie, D.G., Gillis, M.D.D., 1995. Forest inventory in Canada with emphasis on map production. *For. Chron.* 71, 74–88.
- Liaw, A., Wiener, M., 2002. Classification and regression by randomForest. *R News* 2, 18–22.
- Lim, K., Treitz, P., Wulder, M.A., St-Onge, B., Flood, M., 2003. LiDAR remote sensing of forest structure. *Prog. Phys. Geogr.* 27, 88–106. <https://doi.org/10.1191/030913303pp360ra>.
- Luther, J.E., Fournier, R.A., van Lier, O.R., Bujold, M., 2019. Extending ALS-based mapping of forest attributes with medium resolution satellite and environmental data. *Remote Sensing* 11 (9). <https://doi.org/10.3390/rs11091092>.
- Ma, Y., Wu, H., Wang, L., Huang, B., Ranjan, R., Zomaya, A., Jie, W., 2015. Remote sensing big data computing: challenges and opportunities. *Futur. Gener. Comput. Syst.* 51, 47–60. <https://doi.org/10.1016/j.future.2014.10.029>.
- Magnussen, S., Næsset, E., Gobakken, T., Frazer, G., 2012. A fine-scale model for area-based predictions of tree-size-related attributes derived from LiDAR canopy heights. *Scand. J. For. Res.* 27, 312–322. <https://doi.org/10.1080/02827581.2011.624116>.
- Makela, H., Pekkarinen, A., 2004. Estimation of forest stand volumes by Landsat TM imagery and stand-level field-inventory data. *For. Ecol. Manag.* 196, 245–255. <https://doi.org/10.1016/j.foreco.2004.02.049>.
- Mann, H.B., 1945. Nonparametric tests against trend. *Econometrica* 13, 245–259.
- Masek, J.G., Vermote, E.F., Saleous, N.E., Wolfe, R., Hall, F.G., Huemmrich, K.F., Gao, F., Kutler, J., Lim, T.-K., 2006. A Landsat surface reflectance dataset for North America, 1990–2000. *IEEE Geosci. Remote Sens. Lett.* 3, 68–72.
- Matasci, G., Hermosilla, T., Wulder, M.A., White, J.C., Coops, N.C., Hobart, G.W., Bolton, D.K., Tomalski, P., Bater, C.W., 2018a. Three decades of forest structural dynamics over Canada's forested ecosystems using Landsat time-series and lidar plots. *Remote Sens. Environ.* 216. <https://doi.org/10.1016/j.rse.2018.07.024>.
- Matasci, G., Hermosilla, T., Wulder, M.A., White, J.C., Coops, N.C., Hobart, G.W., Zald, H.S.J., 2018b. Large-area mapping of Canadian boreal forest cover, height, biomass and other structural attributes using Landsat composites and lidar plots. *Remote Sens. Environ.* 209, 90–106. <https://doi.org/10.1016/j.rse.2017.12.020>.
- Meyer, D., Tachikawa, T., Kaku, M., Iwasaki, A., Gesch, D., Oimoens, M., Zhang, Z., Danielson, J., Krieger, T., Curtis, B., Haase, J., Abrams, M., Crippen, R., Carabajal, C., 2011. ASTER global digital elevation model version 2 – summary of validation results. NASA L. Process. Distrib. Act. Arch. Cent. Jt. Japan-US ASTER Sci. Team 1–27. <https://doi.org/10.1017/CBO9781107415324.004>.
- Penner, M., Pitt, D.G., Woods, M.E., 2013. Parametric vs. nonparametric LiDAR models for operational forest inventory in boreal Ontario. *Can. J. Remote. Sens.* 39, 426–443. <https://doi.org/10.5589/m13-049>.
- Peterson, A., 2016. Köppen Climate Types of Newfoundland. (WWW Document).
- Pflugmacher, D., Cohen, W.B., E. Kennedy, R., 2012. Using Landsat-derived disturbance history (1972–2010) to predict current forest structure. *Remote Sens. Environ.* 122, 146–165. <https://doi.org/10.1016/j.rse.2011.09.025>.
- Pflugmacher, D., Cohen, W.B., Kennedy, R.E., Yang, Z., 2014. Using Landsat-derived disturbance and recovery history and lidar to map forest biomass dynamics. *Remote Sens. Environ.* 151, 124–137. <https://doi.org/10.1016/j.rse.2013.05.033>.
- Price, D.T., Alfaro, R.I., Brown, K.J., Flannigan, M.D., Fleming, R.A., Hogg, E.H., Girardin, M.P., Lakusta, T., Johnston, M., Mckenney, D.W., Pedlar, J.H., Stratton, T., Sturrock, R.N., Thompson, I.D., Trofymow, J.A., Venier, L.A., 2013. Anticipating the consequences of climate change for Canada's boreal forest ecosystems. *Environ. Rev.* 21, 322–365. <https://doi.org/10.1139/er-2013-0042>.
- R-Core-Team, 2013. R: A Language and Environment for Statistical Computing.
- Saarela, S., Holm, S., Grafström, A., Schnell, S., Næsset, E., Gregoire, T.G., Nelson, R.F., Ståhl, G., 2016. Hierarchical model-based inference for forest inventory utilizing three sources of information. *Ann. For. Sci.* 73, 895–910. <https://doi.org/10.1007/s13595-016-0590-1>.
- Savage, S.L., Lawrence, R.L., Squires, J.R., Holbrook, J.D., Olson, L.E., Braaten, J.D., Cohen, W.B., 2018. Shifts in forest structure in northwest Montana from 1972 to 2015 using the landsat archive from multispectral scanner to operational land imager. *Forests* 9. <https://doi.org/10.3390/f9040157>.
- Strunk, J.L., Temesgen, H., Andersen, H.-E., Packalen, P., 2014. Prediction of forest attributes with field plots, Landsat, and a sample of lidar strips: a case study on the Kenai Peninsula, Alaska. *Photogramm. Eng. Remote Sensing* 80, 143–150. <https://doi.org/10.14358/PERS.80.2.143>.
- Tomalski, P., Coops, N., Marshall, P., White, J., Wulder, M., Bailey, T., 2018. Combining multi-date airborne laser scanning and digital aerial photogrammetric data for forest growth and yield modelling. *Remote Sens.* 10, 347. <https://doi.org/10.3390/rs10020347>.
- Tomppo, E., Olsson, H., Ståhl, G., Nilsson, M., Hagner, O., Katila, M., 2008. Combining national forest inventory field plots and remote sensing data for forest databases. *Remote Sens. Environ.* 112, 1982–1999. <https://doi.org/10.1016/j.rse.2007.03.032>.
- Treitz, P., Lim, K., Woods, M., Pitt, D., Nesbitt, D., Etheridge, D., 2012. LiDAR sampling density for forest resource inventories in Ontario, Canada. *Remote Sens.* 4, 830–848. <https://doi.org/10.3390/rs4040830>.
- Wang, T., Hamann, A., Spittlehouse, D., Carroll, C., 2016. Locally downscaled and spatially customizable climate data for historical and future periods for North America. *PLoS One* 11. <https://doi.org/10.1371/journal.pone.0156720>.
- White, J.C., Wulder, M.A., Varhola, A., Vastaranta, M., Coops, N.C., Cook, B.D., Pitt, D., Woods, M., 2013. A best practices guide for generating forest inventory attributes from airborne laser scanning data using an area-based approach. *For. Chron.* 89, 722–723. <https://doi.org/10.5558/tfc2013-132>.
- White, J.C., Wulder, M.A., Luther, J.E., Hermosilla, T., Griffiths, P., Coops, N.C., Hall, R.J., Hostert, P., Dyk, A., Guindon, L., 2014b. Pixel-based image compositing for large-area dense time series applications and science. *Can. J. Remote. Sens.* 40, 192–212. <https://doi.org/10.1080/07038992.2014.945827>.
- White, J.C., Tomalski, P., Vastaranta, M., Wulder, M.A., Saarinen, S., Stepper, C., Coops, N.C., 2017a. A model development and application guide for generating an enhanced forest inventory using airborne laser scanning data and an area-based approach. In: CWFC Information Report FI-X-018. Canadian Forest Service, Pacific Forestry Centre, Victoria, BC, Canada. <https://doi.org/10.5558/tfc2013-132>. 38 pp.
- White, J.C., Wulder, M.A., Buckmaster, G., 2014a. Validating estimates of merchantable volume from airborne laser scanning (ALS) data using weight scale data. *For. Chron.* 90, 378–385. <https://doi.org/10.5558/tfc2014-072>.
- White, J.C., Wulder, M.A., Hermosilla, T., Coops, N.C., Hobart, G.W., 2017b. A nationwide annual characterization of 25 years of forest disturbance and recovery for Canada using Landsat time series. *Remote Sens. Environ.* 194, 303–321. <https://doi.org/10.1016/j.rse.2017.03.035>.
- White, Joanne C., Coops, Nicholas C., Wulder, Michael A., Vastaranta, Mikko, Hilker, Thomas, Tomalski, Piotr, 2016. Remote Sensing Technologies for Enhancing Forest Inventories: A Review. *Canadian Journal of Remote Sensing* 42 (5), 619–641. <https://doi.org/10.1080/07038992.2016.1207484>.
- Wiken, E.B., Gauthier, D., Marshall, I., Lawton, K., Hirvonen, H., 1996. A Perspective on Canada's Ecosystems: An Overview of the Terrestrial and Marine Ecosystems. Occasional Paper No. 14. Canadian Council on Ecological Areas (CCEA), Ottawa, Ontario.
- Wilkes, P., Jones, S.D., Suarez, L., Mellor, A., Woodgate, W., Soto-Berelov, M., Haywood, A., Skidmore, A.K., 2015. Mapping forest canopy height across large areas by upscaling ALS estimates with freely available satellite data. *Remote Sens.* 7, 12563–12587. <https://doi.org/10.3390/rs70912563>.
- Wulder, M.A., Coops, N.C., 2014. Make Earth observations open access freely available satellite imagery will improve environmental monitoring. *Nature* 513, 30–32.
- Wulder, M.A., Campbell, C., White, J.C.C., Flannigan, M., Campbell, I.D.D., 2007. National circumstances in the international circumboreal community. *For. Chron.* 83, 539–556.
- Wulder, M., White, J.C., Goward, S.N., Masek, J.G., Irons, J.R., Herold, M., Cohen, W.B., Loveland, T.R., Woodcock, C.E., 2008. Landsat continuity: issues and opportunities for land cover monitoring. *Remote Sens. Environ.* 112, 955–969. <https://doi.org/10.1016/j.rse.2007.07.004>.
- Wulder, M.A., Masek, J., Cohen, W., Loveland, T., Woodcock, C., 2012. Opening the archive: how free data has enabled the science and monitoring promise of Landsat. *Remote Sens. Environ.* 122, 2–10. <https://doi.org/10.1016/j.rse.2012.01.010>.
- Wulder, M.A., Coops, N.C., Roy, D.P., White, J.C., Hermosilla, T., 2018. Land cover 2.0. *Int. J. Remote Sens.* 39, 4254–4284. <https://doi.org/10.1080/01431161.2018.1452075>.
- Zald, H.S.J., Wulder, M.A., White, J.C., Hilker, T., Hermosilla, T., Hobart, G.W., Coops, N.C., 2016. Integrating Landsat pixel composites and change metrics with lidar plots to predictively map forest structure and aboveground biomass in Saskatchewan, Canada. *Remote Sens. Environ.* 176, 188–201. <https://doi.org/10.1016/j.rse.2016.01.015>.
- Zhu, Z., 2017. Change detection using landsat time series: a review of frequencies, pre-processing, algorithms, and applications. *ISPRS J. Photogramm. Remote Sens.* 130, 370–384. <https://doi.org/10.1016/j.isprsjprs.2017.06.013>.
- Zhu, Z., Woodcock, C.E., 2014. Automated cloud, cloud shadow, and snow detection in multitemporal Landsat data: an algorithm designed specifically for monitoring land cover change. *Remote Sens. Environ.* 152, 217–234. <https://doi.org/10.1016/j.rse.2014.06.012>.